CHAPTER 3

EXPERIMENTAL AND EMPIRICAL STUDIES

3.1 Introduction

According to the literature survey, maximum research for scour around spur dykes in hydraulics is done on the straight channel at an angle of 90°, 180° channel bend. On behalf of literature, it is concluded that minimal focus is given to the other type of channels such as sinusoidal channel, meandering channel, and other. For enhancing the knowledge to understand the meandering channel, a detailed experiment is performed to examine the scour around the T-shape spur dyke at 180° channel bend under subcritical flow conditions. This chapter also discusses the parameters such as the Froude number of approach flow, the spur dyke in the meander, and the time duration for equilibrium scouring. Further, the non-dimensional empirical equations to predict the temporal and maximum local scour depth are developed. The result of the experiment would also validate by using appropriate pre-existing data.

3.2 The equilibrium scour depth

Many relations and formulae have been developed to estimate the maximum scour depth of the channel. The formulae and relation for estimation can be grouped in following four categories: (1) Regime approach (relate the scour depth with increased discharge intensity), (2) Dimensional analysis approach (mainly deals with field data or the experiment data), (3) Analytical and semi-analytical approach, (4) The Probabilistic approach. The present work is related to a dimensional analysis-based approach to estimate the maximum scour depth

3.2.1 Dimensional Analysis and similitude

A physical model gives more accuracy in its result only when the model is appropriately designed. The correct approximation of physical process is given by a small-scale representation of the real process if the two are related (Yalin, 1989). The scaling law and different similitude in the physical model have been described on several occasions, for example (Hugues (1993); Ettema et al., 2000; Heller et al., 2007).

Similitude or scaling laws are some formal features satisfied by the scale in between the prototype and model to achieve similarity. Several classes of similitude are present but here we will be discussing only the similitude by dimensional analysis.

3.2.2 Temporal Variation of scour depth

According to Kothyari and Ranga, (2001),the time required for a given scour discharge to its full potential is much larger than the time required for its run. So, the temporal variation of scouring has great significance, particularly for predicting the scour in rivers where flow is unsteady, and discharge can change rapidly.

Masjedi et al., (2010a) studied the time required to develop local scours in spur dyke at 180^0 flume bend and the effects of various flow intensities (V*/V*c) on the temporal development of scour depth at the spur dyke. The study shows that the maximum depth of scouring is dependent upon the experimental time. As the flow velocity increases, the scour will also increase.

3.3 General Equations for maximum local scour in meandering channel

The local scour around T-shaped spur dyke placed in a channel bend depends upon (1) geometry of the channel (width, radius, and bed-slope); (2) spur dyke characteristics (its length and wing length, inclination with the bank, and location in the channel); (3) approach flow conditions (depth, discharge rate and velocity of flow); (4) properties of

the bed sediment (specific gravity, grain size, friction angle); (5) properties of the flowing fluid (its density and viscosity); and (6) time duration. Hence, the scour depth can be expressed as;

$$d_s = f(L, l, \alpha, \theta, y, W, S_0, V, g, d_{50}, R_c, \rho_s, \emptyset, \rho, \mu, t, t_e) \tag{3.1}$$

Where d_s is temporal (time-varying) scour depth; L, l are the length and the wing length of the spur dyke respectively;α is the angle of spur dyke with the bank; θ is the location of spur dyke in bend measured from the entry to the bend; y and V are the depth and velocity of approach flow; W is the channel width; S_0 is bed slope; g is the gravitational acceleration; d_{50} is median grain size; R_c is the central radius of the bend; ρ_s is the density of sediment; μ is the dynamic viscosity of the flowing fluid; $\emptyset$ is friction angle of sediment; t is the time of scouring; and t_e is the time taken to reach maximum (or equilibrium) scour depth.

Using dimensional analysis, Equation (3.1) can be written in a non-dimensional form as;

$$\frac{\mathrm{d_s}}{\mathrm{y}} = \mathrm{f}\left(\mathrm{Re}, \mathrm{Fr}, \frac{\theta}{180}, \alpha, \mathrm{S_0}, \emptyset, \frac{L}{R_c}, \frac{\mathrm{d_{50}}}{y}, \frac{\mathrm{L}}{\mathrm{W}}, \frac{\mathrm{l}}{\mathrm{L}}, \frac{\mathrm{L}}{\mathrm{d_{50}}}, \frac{\rho_\mathrm{s}}{\rho}, \frac{R_c}{\mathrm{W}}, \frac{\mathrm{t}}{\mathrm{t_e}}\right) \tag{3.2}$$

Here, Fr and Re are Froude numbers and Reynold's number related to approach flow, respectively. In this study, it is assumed that Fr , θ (in degree) and t/t_e are only influencing parameters, as these are the only parameters that change during the experimental run (discussed in the previous section); all other parameters are either constant or assumed to have a negligible effect on the scouring phenomenon. Therefore, Equation (3.2) can be simplified as:

$$\frac{\mathrm{d_s}}{y} = f\left(\mathrm{Fr}, \frac{\theta}{180}, \frac{t}{t_e}\right) \tag{3.3}$$

The geometry of scour around a T-shaped spur dyke in bend mainly depends upon channel geometry such as bed slope, radius, and width of the channel, and also in spur dyke characteristics like (length and wing of spur dyke, angle, and location of the bend), the flow conditions (approach depth and velocity), sediment properties such as specific gravity, grain size, friction angle and fluid parameters like density and viscosity. Hence the depth of scouring d_s is;

$$ds = f(L, l, \alpha, \theta, y, B, S_0, V, g, d_{50}, R, \rho_s, \emptyset, \rho, \mu, t) \quad (3.4)$$

here *L* = length of spur dyke, l = wing of spur dyke, and θ = an angle of spur dyke with bank,α = location of spur dyke in bend, y = approach flow depth, B = channel width, is S_0 = bed slope, V = approached flow velocity, g = gravitational acceleration, d_{50} = median grain size, R = radius of bend, ρ_s = density of sediment, $\emptyset$ = viscosity of the fluid, ρ = friction angle of sediment, t = time of scour. By using the dimensional analysis, above Equation (3.4) can be written as;

$$\frac{ds}{y} = f\left(Fr, \theta, \alpha, S_0, \emptyset, R_e, \frac{L}{B}, \frac{l}{L}, \frac{L}{d_{50}}, \frac{\rho_s}{\rho}, \frac{R}{L}, \frac{t}{t_e}\right) \quad (3.5)$$

Where Fr = Froude number, Re, = Reynolds number, and t_e = maximum of time development of scour. After simplification of the above equation by eliminating constant the new equation may be written as;

$$\frac{ds}{y} = f\left(Fr, \frac{\theta}{180}, \frac{t}{t_e}\right) \quad (3.6)$$

3.4 Experimental setup

The experiment was carried out in a Hydraulic and Water Resource Engineering Laboratory, Department of Civil Engineering at IIT BHU located in Varanasi. The experiment includes a meandering channel with a rectangular cross-section. Having two

bends of reverse order (θ_c=180°) can be clearly shown in Figure 3.1 and a cross-section of the channel represented in Figure 3.2.

To obtain the maximum deflection of the flow, the central angle of the bend was kept 180^0. The width of the channel and central radius of the bend is 1.0 m, The floor and wall of the rectangular channels were made impermeable with the plastering of cement mortar. The two consecutive bends are connected to both straight inlet and outlet channels of the flume every 6 m in length.

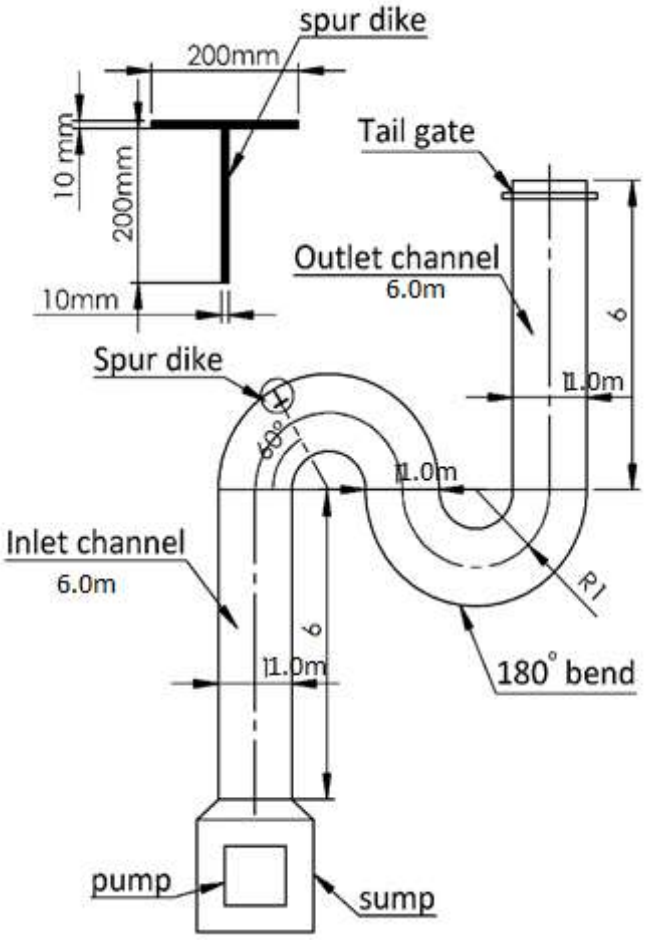

Figure 3.1 A schematic diagram of the reverse bend rectangular meander channel

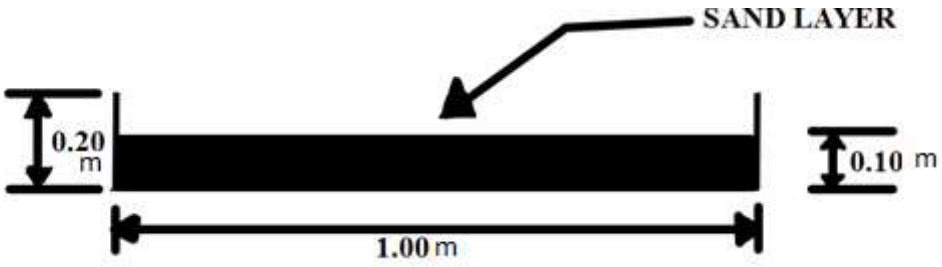

Figure 3.2 Cross-section of channel

A tailgate was present at the end of the exit channel for controlling the flow depth of the stream. A sharp-crested rectangular weir is at the end of the side-channel, located after the tail gate is used for measuring the discharge. Outflow from the side channel joins the sump well. The water is pumped from the sump well into the inlet chamber, which joins the inlet channel. The relative curvature of bend is $(R_c/B) = 1$, representing a sharp bend.

3.4.1 Measuring Equipment

The following measuring equipment has been used for the measurements of different flow parameters of interest:

3.4.1.1 **Point gauge**

A Point gauge is used to measure water surface elevation and channel bed level with an accuracy of ±0.1 mm.

3.4.1.2 **Current meter**

The PYGMY type current meter is scaled two-fifths as large as the standard type current meter; it does not have a tailing assembly. Its range of operation is 0.3 to 3.3 m per second. This microcontroller-based water velocity indicator has been designed to measure water velocity in the flowing stream. It contained the latest microchip micro-controller and can be used with any calibrated water current meter. The one pulse per resolution signal obtained from the current meter is processed internally, and a microcontroller compatible signal is generated. These signals are evaluated against time signals which are

generated through a crystal-controlled precise clock. Finally, the water velocity is analysed as per the calibration equation through software and display on a 16×2 LCD. The velocity indicator consists of 4 switches mounted on the front panel, one each for function/Esc, Up, Down, and save/enter/power on. Two terminals to connect the current meter sensor are also provided on the top, and one power connector for charging, as shown in Figure 3.3.

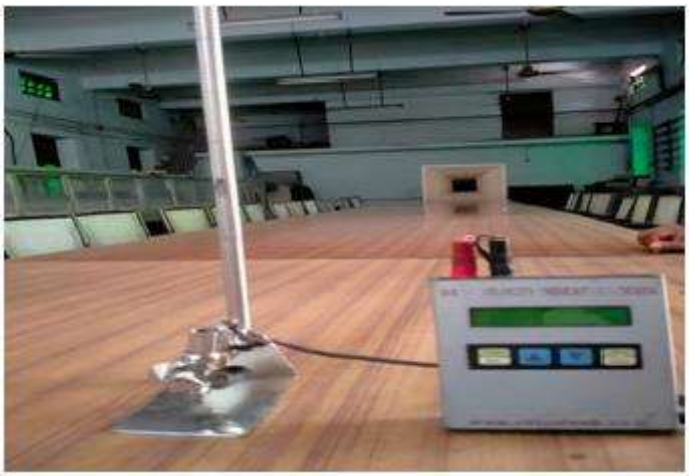

Figure 3.3 current meter

3.4.2 Geometry of T-shaped Spur Dyke used in the Experiment

For this experiment, the spur length and wing length are 20 % of the channel width shown in Figure 3.4. The spur dykes were made of Perspex sheet. The entire spur dykes included in the experiment was placed perpendicular to the channel bed.

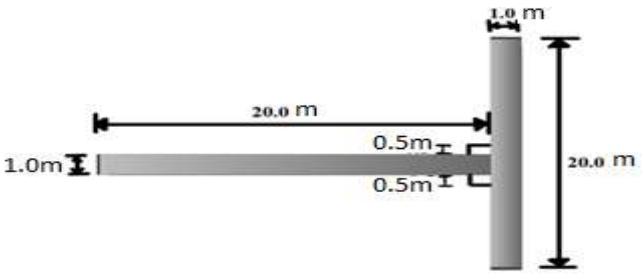

Figure 3.4 Plan of T-shape spur dyke

3.5 Procedure

Before the experiment, the T-shape spur dyke model is placed on the sediment bed surface and the bed levelled with a scraper blade mounted on a carriage that rode on the steel rods after the bed was completely wetted and drained Figure 3.5.

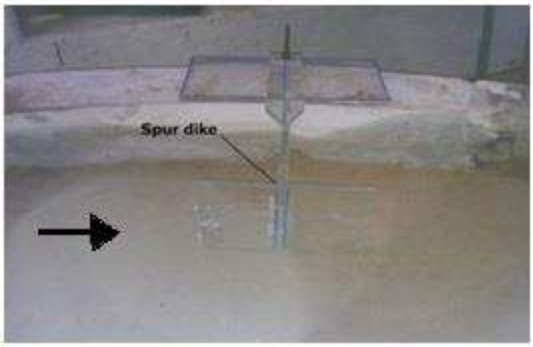

Figure 3.5 Placement of T-shaped spur dyke at 60° location in a laboratory channel

After this, the flume was filled with water and obtained the desired depth. Before starting the pump, an initial set of a transect of the anticipated scour region was collected. The pump was shut down on completing each test and the flume was allowed to drain out slowly without any disturbance in the bed's topography. The flume bed was allowed to dry and the final maximum scour depth was recorded using the point gauge. At maximum scour, the depth of scour does not change with time. The experiment was considered with spur dyke having l/L=1, with different Froude numbers and 30°, 60°, 120°, and 150° with scouring depth measured. Experiments were conducted under clear water scour regime for 24 hours, so the moment of sediment was almost negligible and attained the equilibrium state of scouring. The results are shown that the 93% scour occurs during the first three hours. Hence, three-hour duration was selected for each test. Uniform sediment with a median size of d_{50} = 2 mm and geometric standard deviation σ_g = 1.7, used thickness of 0.2 m and covered the total length of the channel shown in Figure 3.6.

a. Preparation of bed surface

b. Placing of T shape spur Dyke

c. The initial stage of the flow

d. The final stage of scouring

Figure 3.6 Meandering channels

After setting the proper infrastructure of the channel, the experiment was conducted in a meandering channel with a rectangular cross-section and two consecutive bends of reverse order. These consecutive bends were connected with the straight inlet and outlet channels, each of length 6.0 m Figure 3.1. The width of the channel cross-section was kept uniform, equal to 1.0 m. The central radius of both bends was designed as 1.0 m. The bend is categorized as a sharp bend because of the value, R_c/W, i.e., the relative curvature, was 1.0. The central angle of the bend was kept 180° for the maximum deflection of flow and hence, to generate maximum development of secondary circulation.The floor and the wall of the rectangular channel were made impermeable by plastering with cement mortar. A 0.25 m thick layer of bed sediment, having a median

diameter, d_{50}= 2 mm and standard deviation, σ_g= 1.8 was uniformly distributed throughout the channel.

The spur dyke having a thickness of 10 mm and height of 200 mm, was made of a perspex sheet and was placed perpendicular to the curvature of the flume bend. The length and the wing length of the spur dyke were taken as 20% (i.e. 200 mm) of the width of the channel.

At the end of the outlet channel, a tailgate was installed to maintain flow depth in the channel. The water came out from the main channel's exit, and the sharp crest rectangular weir equipped this position for measuring the flow discharge. A centrifugal pump was connected to the channel through which water goes back to the pump well. The channel bed was labeled using a scraper blade in each run, and the flume was filled with water up to its required depth. Before starting the pump, the initial setup channel bed elevation values where the scour expected to form were measured and calculated. After running, the water in the flume was drained out slowly without much affecting the bed topography and the setup was left to dry. A picture of the scour topography around the spur dyke was taken.The accuracy of the used point gauge is ±0.01 mm. The experiment was conducted for the spur dyke located in the first bend at the angle of 30^o, 60^o, 120^o, and 150^o (measured from the entry to the bend). A schematic diagram for the spur dyke placed at 60^o shown in Figure 3.6d for each location, the experiment runs for four different discharge values (or Froude number).

It should be noted that the experiment was conducted under clear-water conditions and sub-critical approach flow conditions. A preliminary experimental run was conducted for five hours, and the change in bed elevation at the location of maximum scour becomes negligible. A similar observation is made by (Masjedi et al., 2010a, 2010b, 2010c, 2011).

3.6 Results and discussions

3.6.1 Flow characteristics in general

To visualize the surface flow structure around the spur dyke at the maximum scour condition, tracers were used. As expected, the restriction to flow caused by spur dyke results in three different zones in the region surrounding the spur dyke. These three zones are the main channel zone, an embayment zone, and a mixing zone (Zhang and Nakagawa, 2008; Pandey et al. 2018). The main channel zone spans from the wing of spur dyke to the opposite inner bank of the channel, embayment zone located between the wing of spur dyke and outer bank from where the structure is protruded, and mixing zone in between the two. It was observed that when the flow approaches the spur dyke, a strong inward circulation is generated with the increase in spur dyke's location from the entry of bend, the length of flow separation, and hence, embayment zone increases. It occurs due to the diversion of streamline flow caused by the curvature of the bend. The flow velocity was found to be decreasing in the embayment zone. Here, the tracers representing the central area of the embayment were observed to be diverted in three directions; downstream, upstream, and towards the main channel. Hence, it can be concluded that the flow pattern around the spur dyke is very complicated and strongly three-dimensional. It may occur due to the formation of the degraded bed surface.

3.6.2 Bed Topography

The artificial narrowing created in the main channel caused by the spur dyke results in flow disturbances around the structure. It was observed that the two main scour holes' form; one at upstream forms near the nose (or wing of spur dyke), and the other at downstream forms in the embayment area at a distance from the spur dyke, as can be seen in Figure 3.7 As the spur dyke shifts to the end of the first bend, the scour area at upstream stretches along the wing of the spur dyke and merges with the scour area

downstream. The sediment erosion in the embayment area suggests that there are strong return currents generated in this area. Because of the diverted flow generating at the head of the spur dyke, various local scour is formed in front of the structure. These scour holes started forming as soon as the pump was started. In general, it was observed that sediment erosion takes place at the outer bank while deposition occurs at the inner bank. In the case of spur dyke placed at θ = 30^o, the deposition occurs nearly throughout the length of the inner bank (of the first bend), as shown in Figure 3.7a.

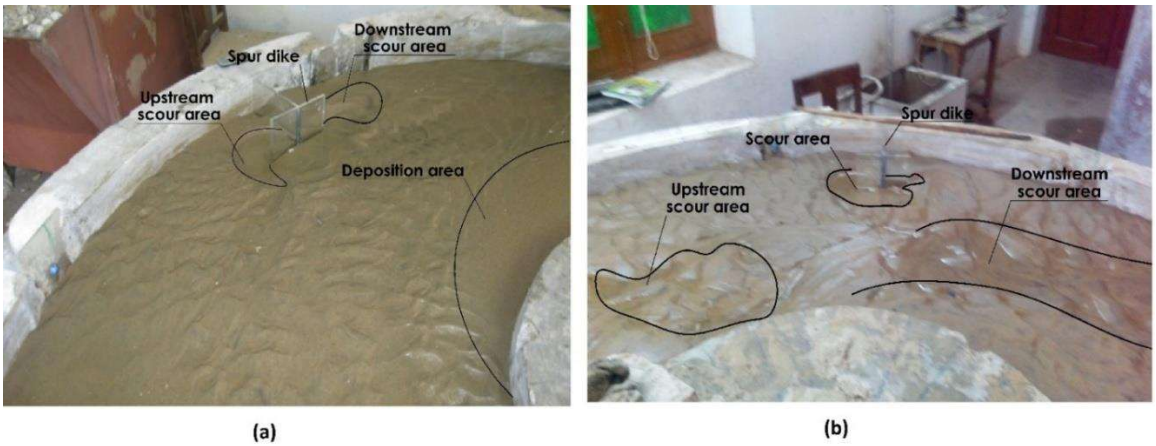

Figure 3.7 Bed topography for spur located at (a) θ = 30^o; and (b) θ = 120^o

For θ = 120^o and 150^o, the scour area extends to the main channel (closer to the inner bank) as well, shown in Figure 5.3b. In the case of θ = 120^o, the increase in turbulent and secondary flow caused due to change in the curvature of the bend results in severe scour in the main channel, both upstream and downstream, resulting in extensive bed degradation as shown in Figure 6.1b. Interestingly, the scour area formed upstream is bounded and located far from the structure. Due to the sharp change in the channel curvature, it might occur, creating a high secondary and spiral flow, followed by backwater formation caused by spur dyke resulting in the generation of high turbulence region at the upstream side. The increased velocity of diverted flow associated with high turbulence at downstream results in scouring near the tip of the spur dyke's wing, which extends in an elongated fashion or pattern. Since the only tracer has been used to study

the surface flow characteristics, the exact reason behind such scours is not identified. Hence, it can be treated as an experimental limitation. A highly advanced setup to observe the flow field is required. It was seen that with increasing discharge (or Froude number), flow is attracted towards the spur dyke, which causes scour near the nose of the wing (at upstream). With the increase in Froude number, general scour in the channel reduces and shifts towards spur dyke, while the main scour hole depth increases, as shown in Figure 3.8. A general scour contour for Fr = 0.35 and Fr = 0.50 is shown in Figure 3.8 for spur dyke placed at $\theta = 30^{o}$. From Figure 3.8, it can be seen that the overall bed elevation in the main channel zone decreases with the increase in the Froude number (from 0.35 to 0.50). From Figure 3.8b, it can be seen that at a higher Froude number, the local scour hole upstream of the spur dyke extends to merge with the scour hole downstream. This phenomenon might be the consequence of the formation of large vortices around the wing of the spur dyke.

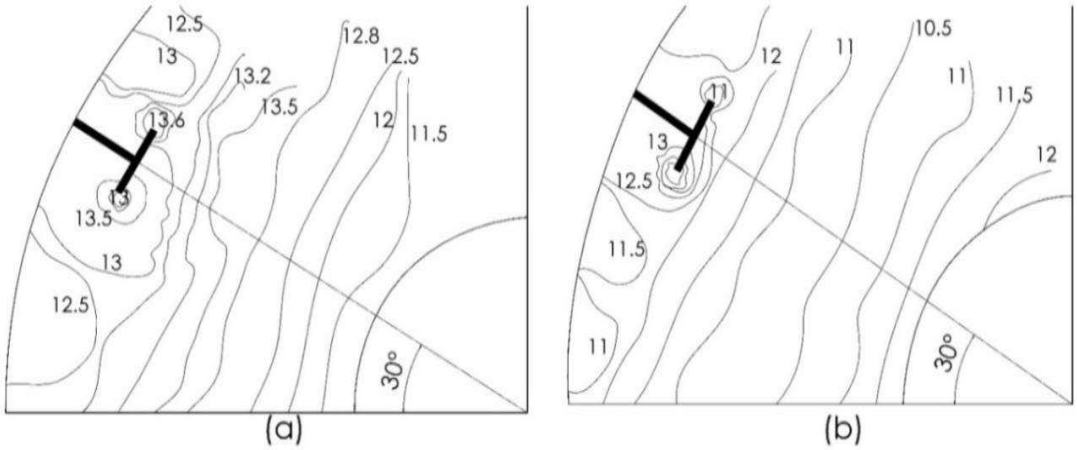

Figure 3.8 Scour contour around spur dyke located at θ = 30°, (a) Fr = 0.35; and (b) Fr = 0.50.

3.6.3 Temporal and maximum scour depth

In general, scour increases rapidly at the earlier stage of its development and then gradually grows at a decreased rate, reaching its maximum value after sometime. The time-varying scour depth for each location of spur dyke in the channel is shown in Figure

3.9. The figure shows that a considerable amount of scour depth (nearly 90% of maximum scour depth) is reached within 20% of experimental duration except in few cases. A similar finding was made by several other researchers, such as (Pu and Lim, 2014). The temporal scour depth variation shows logarithmic incremental behaviour (Coleman et al., 2013; Kothyari et al., 2007).

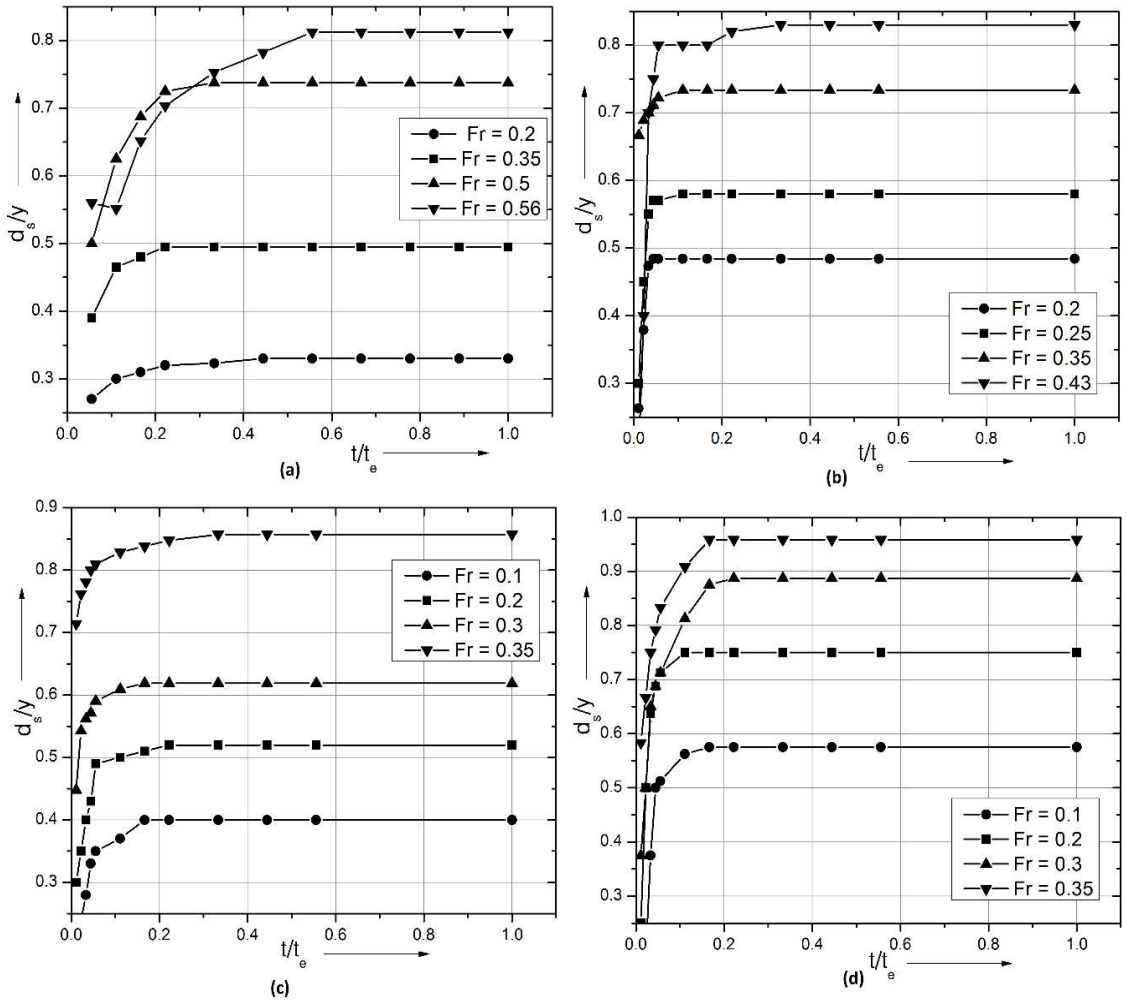

Figure 3.9 Temporal scour depth variation for spur dyke located at θ = 30°, 60°, 120°, and 150°, respectively

From Figure 3.9a, it is interesting to note that the transition stage (curvy region) of scour development is well defined and steady (or smooth) for spur dyke located at θ = 30°. The transition stage becomes sharp (or unsteady) as the location of the spur dyke shifts towards the end of the first bend. It can be concluded from the graph that for each

location of spur dyke, the temporal scour depth increases with an increase in Froude number.

For the spur dyke located at θ = 120^o and 150^o, the local scour was very high even for approach flow with a low Froude number. It was found that for θ = 150^o and Fr = 0.10, the maximum non-dimensional scour-depth value is 0.58, which is close to the value for θ = 60^o and Fr = 0.25. The region around the bend is most affected by scouring. This may occur due to a change in the curvature of the meandering channel (or inflection point) downstream.

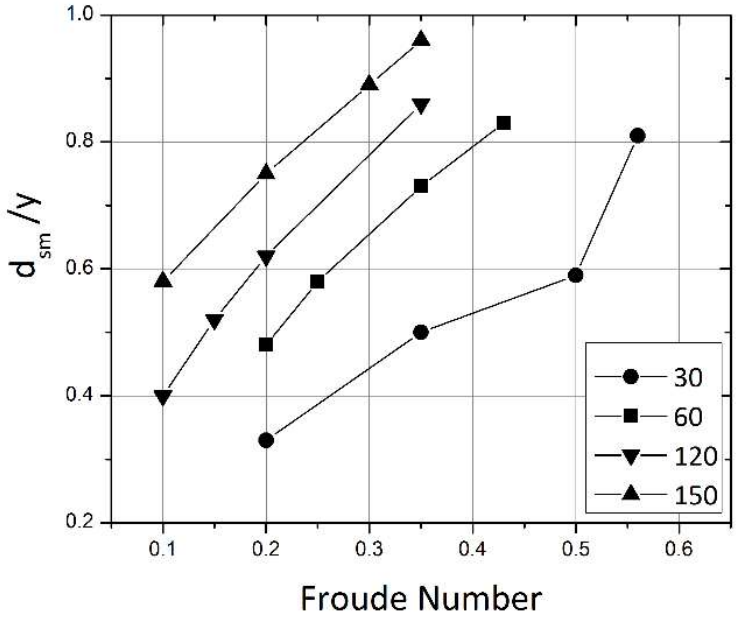

Figure 3.10 Variation of ds_m/y with Froude number for different locations of spur dyke

From Figure 3.10, it can be concluded that for the constant value of Froude number (i.e.,r = 0.20 and 0.35), the initial growth rate of scour depth increases as the spur dyke shifts towards the end of the first bend. In addition, the maximum scour depth also increases with an increase in the Froude number and location of spur dyke shown in Figure 3.10-3.11.

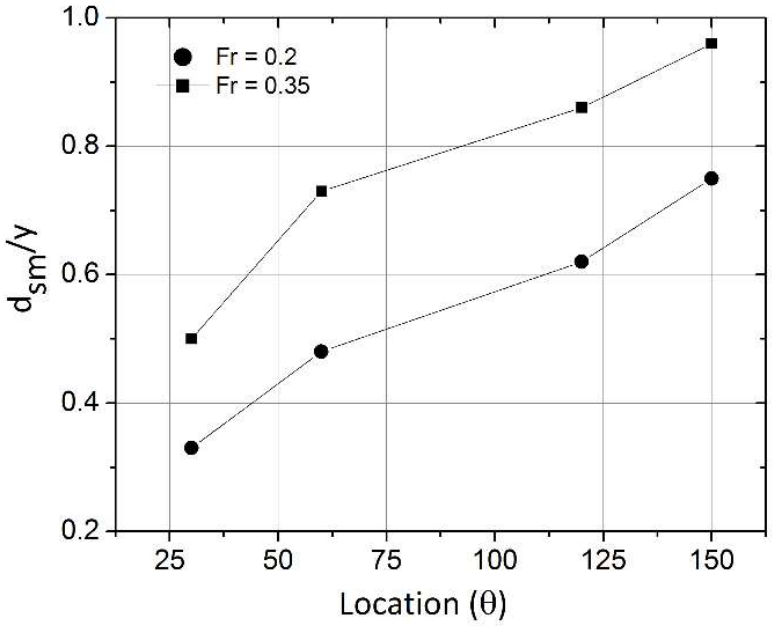

Figure 3.11 Variation of ds_m/y Vs. θ

3.6.4 Mathematical formulation for temporal and maximum scour depth

Since the scour depth shows logarithmic incremental variation, Equation in non-dimensional form can be written in the following empirical form;

$$\frac{d_s}{y} = a \cdot Fr^b \left[\frac{\theta}{180^0}\right]^c ln\left[\frac{t+t_e}{t_e}\right] \tag{3.7}$$

The constants a, b, c are determined by the method of best-fit using the experimental data. The resulting best-fit equation comes out as;

$$\frac{d_s}{y} = 2.747 \cdot Fr^{0.574} \left[\frac{\theta}{180^0}\right]^{0.381} ln\left[\frac{t+t_e}{t_e}\right] \tag{3.8}$$

The maximum scour depth, d_{sm} is reached at $t = t_e$. And hence, Eq. 3.8 is reduced to;

$$\frac{d_{sm}}{y} = 1.904 \cdot Fr^{0.574} \left[\frac{\theta}{180^0}\right]^{0.381} \tag{3.9}$$

Equation (3.8) and Equation (3.9) show self-similarity. Equation (3.9) is used to estimate the maximum scour depth and then compared with the measured data.

3.7 Validation results

The developed equation for scouring shows good accuracy when compared with experimental data having R^2 = 0.895 and percentage error ranging between 1.28% to 18.33%, as can be shown in Figure 3.12. Therefore, it can be expected that the relationship derived is good for the given range of Froude numbers.

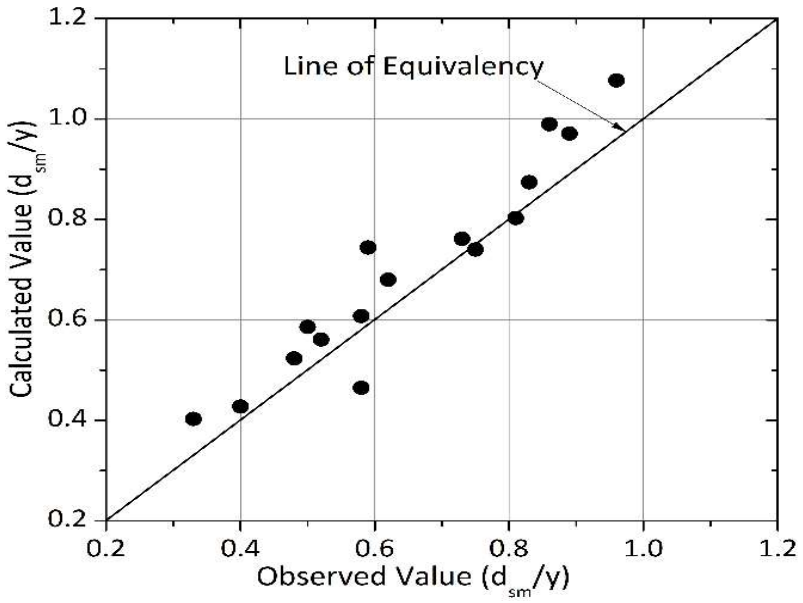

Figure 3.12 Comparison of the calculated and observed value of maximum scour depth

To check the applicability of the proposed equation on other conditions, experimental data from Masjedi et al. (2010b, 2010c, and 2011) were used to conduct the experimental investigation on scour around the T-shaped spur Dyke placed in an 180^o bend. This attempt assuming that the downstream flow characteristic has a negligible effect on maximum scour depth. Since the bend angle in all three cases is 180^o, it is presumed that the proposed equation could give reasonable results. It is found that the proposed equation overestimates the maximum scour depth, nearly by an average factor of 1.19, 1.41, and 2.2 respectively shown in Figure 3.13.

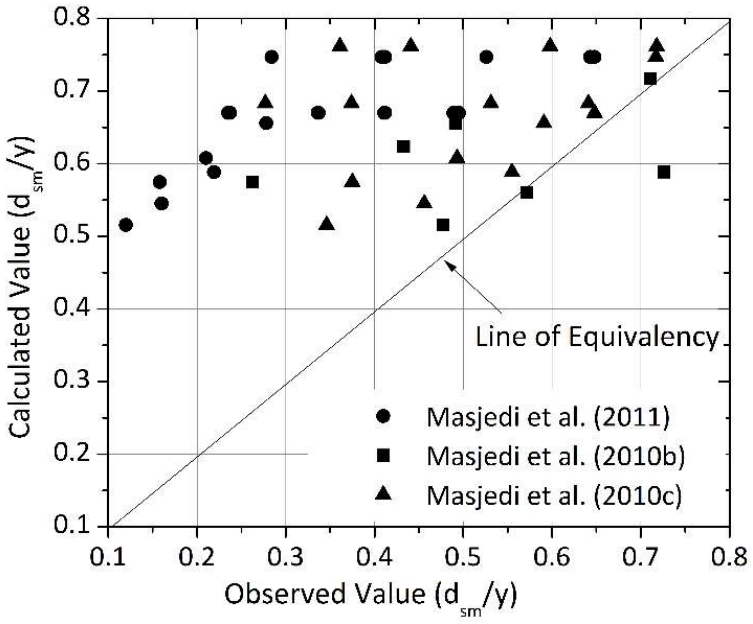

Figure 3.13 Comparison of the calculated and observed value of maximum scour depth (from other result.)

This may occur due to various other influencing parameters assumed to be constant or have a negligible effect. Therefore, it is recommended to encompass various other parameters in developing such an empirical equation.

3.8 Conclusion

The experiment was set up to investigate the flow field and scour depth in the area surrounding a spur dyke placed at various locations in a reverse meandering channel. The reverse meandering channel enables maximum deflection of the flow field and generates high turbulence and secondary flow conditions to simulate the maximum amount of scour around a spur dyke. This study would be helpful as an engineering application in a river channel where the last stage of meandering is almost reached (i.e., before forming an ox-bow lake). Vortex flow was observed at the beginning of each experimental run, due to which a secondary current was created. The secondary flow transports the sediments towards the convex side (inner bank), creating a few dunes near the inner wall. It can be concluded that the local scour holes formed might extend to the river banks in case of a

high flow discharge rate (or Froude number). This could be attributed to the existence of return currents towards the river banks generated when the flow is diverted from the heads of the spur dykes. This further resulted in the sound degradation of the main channel near the spur dyke. From an engineering perspective, this is a significant drawback. If appropriate countermeasures are not taken, then both the river bank and structure are at risk. It may lead to failure and then collapse of the structure. It was observed that the maximum scour depth increases with an increase in the Froude number and location of the spur dyke from the entry of the bend. The temporal variation of scour depth with time shows a logarithmic trend. Empirical relations for temporal and maximum scour depth are established as a function of the Froude number and the position of the structure in the bend. The developed equation shows good accuracy when compared with (own) experimental data. However, it overestimates the maximum scour depth for experimental data (related to 180° channel bend) from the literature. This discrepancy could be the result of the negligence of several parameters that affect the scour depth. In addition, the range of the Froude number of the approach flow is kept narrow due to experimental setup constraints. In the future scope of studies, it is advised to incorporate various parameters that influence the scour, such as the dimensions of the spur dyke, channel parameters, and so on, and to run experiments for a wide range of Froude numbers. Since the experimental study is limited to very few parameters, it should not be used for engineering purpose and design of other hydraulic structures without verification.

In this study, only tracers were used to carry out a qualitative assessment of the surface flow field, which is very limited to a greater extent. In future studies, it is recommended to include a quantitative assessment of the flow field around the structure. The study can be further carried out for simultaneous positioning of a spur dyke at different locations on

the concave side of the meandering channel. At a later stage, the study can also be incorporated with numerical investigation or modelling.